


# Tissue-Engineered Human Myobundle System as a Platform for Evaluation of Skeletal Muscle Injury Biomarkers

Alastair Khodabukus ,\* Amulya Kaza,\* Jason Wang,\* Neel Prabhu,\* Richard Goldstein,<sup>†</sup> Vishal S. Vaidya,<sup>†</sup> and Nenad Bursac<sup>\*,1</sup>

\*Department of Biomedical Engineering, Duke University, Durham, North Carolina 27708-90281; and <sup>†</sup>Drug Research and Development, Pfizer, Groton, Connecticut 06340

Alastair Khodabukus and Amulya Kaza contributed equally to this study.

The authors certify that all research involving human subjects was done under full compliance with all government policies and the Helsinki Declaration.

<sup>1</sup>To whom correspondence should be addressed at Department of Biomedical Engineering, Duke University, 101 Science Drive, FCIEMAS 1427, Durham, NC 27708-90281. Fax: (919) 684-4488. E-mail: nbursac@duke.edu.

## ABSTRACT

Traditional serum biomarkers used to assess skeletal muscle damage, such as activity of creatine kinase (CK), lack tissue specificity and sensitivity, hindering early detection of drug-induced myopathies. Recently, a novel four-factor skeletal muscle injury panel (MIP) of biomarkers consisting of skeletal troponin I (sTnI), CK mass (CKm), fatty-acid-binding protein 3 (Fabp3), and myosin light chain 3, has been shown to have increased tissue specificity and sensitivity in rodent models of skeletal muscle injury. Here, we evaluated if a previously established model of tissue-engineered functional human skeletal muscle (myobundle) can allow detection of the MIP biomarkers after injury or drug-induced myotoxicity *in vitro*. We found that concentrations of three MIP biomarkers (sTnI, CKm, and Fabp3) in myobundle culture media significantly increased in response to injury by a known snake venom (notexin). Cerivastatin, a known myotoxic statin, but not pravastatin, induced significant loss of myobundle contractile function, myotube atrophy, and increased release of both traditional and novel biomarkers. In contrast, dexamethasone induced significant loss of myobundle contractile function and myotube atrophy, but decreased the release of both traditional and novel biomarkers. Dexamethasone also increased levels of matrix metalloproteinase-2 and -3 in the culture media which correlated with increased remodeling of myobundle extracellular matrix. In conclusion, this proof-of-concept study demonstrates that tissue-engineered human myobundles can provide an *in vitro* platform to probe patient-specific drug-induced myotoxicity and performance assessment of novel injury biomarkers to guide preclinical and clinical drug development studies.

**Key words:** muscle; tissue engineering; biomarker; statin; toxicity; atrophy; myopathy.

Myopathic diseases result in structural and functional impairment of skeletal muscle that can arise from direct or indirect drug interactions, nutritional defects, toxin exposure, or genetic disorders (Chavez *et al.*, 2016; Goldstein, 2017). Drug-induced myopathies are typically mild and present clinically as myalgia but can lead to rhabdomyolysis resulting in myoglobinuria, renal failure, and in extreme cases death (Chavez *et al.*, 2016;

Torres *et al.*, 2015). Statins are the most prevalent drug family inducing myotoxicity, with cerivastatin being withdrawn from the market due to fatal cases of rhabdomyolysis (Omar and Wilson, 2002; Staffa *et al.*, 2002; Thompson *et al.*, 2003). However, multiple drug families can cause myopathy, including glucocorticoids (Gupta and Gupta, 2013), antimalarials (Casado *et al.*, 2006), and antiretroviral drugs (Dalakas *et al.*, 1990), which

necessitates the development of sensitive and predictive assays for muscle damage.

The ability to noninvasively detect muscle damage would not only lead to prevention of drug-induced myotoxicity but also provide longitudinal assessment of muscle repair and regeneration, ultimately resulting in improved patient safety and therapeutic outcomes. Traditionally, skeletal muscle damage has been assessed by the classical biomarkers creatine kinase (CK), aspartate amino transferase, and to a lesser extent lactate dehydrogenase (LDH) (Goldstein, 2017; Rodrigues et al., 2010). However, these biomarkers are nonspecific to skeletal muscle (Castro and Gourley, 2012; Keltz et al., 2014), lack sensitivity to detect lower grade myopathies (Dabby et al., 2006), and do not correlate with disease severity in genetic myopathies (Govoni et al., 2013; Gunst et al., 1998; Vaananen et al., 1988). This limits their ability to predict drug myotoxicity and to indirectly report drug effects on muscle function and recovery from injury. Recently, a novel skeletal muscle injury panel (MIP) of biomarkers consisting of skeletal troponin I (sTnI), fatty-acid-binding protein 3 (Fabp3), creatine kinase measured by a mass assay (CKm), and myosin light chain 3 (Myl3), has been identified as more specific and predictive of skeletal muscle injury. This biomarker panel has been extensively characterized and validated in rodent models against multiple known myotoxins including statins and clofibrate (Bodie et al., 2016; Burch et al., 2016; Maliver et al., 2017; Tonomura et al., 2012). Encouragingly, the MIP has been recently validated in patients with genetic muscular diseases (Burch et al., 2015; Goldstein, 2017; Hathout et al., 2016b). The ability to develop in vitro human model systems that can serve as a reliable platform for testing muscle injury biomarkers has been important regarding that small animal models are poor predictors of human drug toxicity (Hay et al., 2014) and there may exist potential species-specific differences in biomarker release.

Conventionally, high-throughput drug screens have been facilitated by the use of cultured cells. However, traditional two-dimensional (2D) cell culture models do not support long-term culture of primary contractile myotubes due to their detachment from a dish. Myotube detachment prevents tissue maturation and long-term drug treatments, thus decreasing physiological relevance and predictive power of these systems (Funanage et al., 1992; Khodabukus et al., 2018; Wang et al., 2019). To overcome these limitations, we have developed three-dimensional (3D) engineered skeletal muscle tissues ("myobundles") derived from human primary myogenic progenitor cells (Khodabukus et al., 2019; Madden et al., 2015) or induced pluripotent stem cells (Rao et al., 2018). The myobundle systems support increased culture duration and maturation compared with 2D culture and permit measurements of muscle contractile strength. Importantly, primary human myobundles replicate functional and histopathological responses to various drug classes including statins (Madden et al., 2015; Zhang et al., 2018), the antimalarial chloroquine (Madden et al., 2015), and mitochondrial toxins (Davis et al., 2017). Additionally, tissue-engineered rat skeletal muscle models have been used to study muscle injury and regeneration in vitro (Juhás et al., 2014, 2018; Tiburcy et al., 2019). During the last decade, the ability to perform medium-throughput drug studies in engineered muscles has been aided by their miniaturization and development of automated methods to assess muscle function (Afshar Bakooshi et al., 2019; Mills et al., 2019; Vandenburgh et al., 2008). Furthermore, engineered muscle systems have been made more mimetic by incorporating motor neurons (Afshar Bakooshi et al., 2019; Osaki et al., 2018; Vila et al., 2019), vascular

cells (Bersini et al., 2018; Gholobova et al., 2015; Maffioletti et al., 2018), and immune cells (Juhás et al., 2018). Alternatively, engineered muscle systems can be coupled to additional organ systems to better model human in vivo drug metabolism and generate multi-organ in vitro drug discovery models (Broer et al., 2020; Oleaga et al., 2016; Skardal et al., 2017; Verneti et al., 2017).

Here we performed a proof-of-concept study to investigate if primary human myobundles can be used to study drug-induced myotoxicity and noninvasive detection of injury biomarkers. First, we showed that release of all members of the MIP can be detected upon a supra-physiological injury of myobundles by the snake toxin notexin. We then assessed changes in MIP biomarker release and, myobundle contractile function and structure in response to physiological levels of pharmaceuticals and growth factors known to be myotoxic (ie, cerivastatin and dexamethasone) and non-myotoxic (ie, pravastatin and IGF-1). Although muscle force generation was altered in response to drug treatment as expected, we found that MIP biomarker release did not always correlate with these functional changes and was dependent upon mode of injury. Overall, our studies show that the myobundle system can provide a platform for studying biomarker release, identifying and evaluating novel muscle-specific biomarkers, and predicting human drug toxicity in a patient-specific manner using functional readouts.

## MATERIALS AND METHODS

### Myoblast isolation

Human skeletal muscle samples were obtained through surgical waste from two donors with informed consent under Duke University IRB approved protocols (Pro00048509 and Pro00012628). Muscle samples were minced and digested with 0.05% trypsin for 30 min at 37°C. Isolated cells were centrifuged and resuspended in growth media consisting of low-glucose DMEM (Sigma, D6046), 10% fetal bovine serum (Hyclone, SH3008803, lot no. AD21573306), 10 ng/ml EGF (Prospecbio, CYT-217), 50 µg/ml fetuin (Sigma, F2379), and 0.4 µg/ml dexamethasone (Sigma, D4902). After pre-plating, cells were seeded on Matrigel (BD Biosciences, 354234) coated flasks and expanded by passaging upon reaching 70% confluence. At passage 4, cells were detached by trypsin and used to fabricate myobundles. Cellular composition was assessed by immunostaining of myoblasts with the muscle marker desmin (Abcam, ab32362) and intermediate filament marker vimentin (Abcam, ab92547). Myogenic cell purity, assessed by proportion of desmin positive cells, was not significantly different between donor 1 (68.1 ± 4.6%) and donor 2 (73.4 ± 5.2%).

### Myobundle fabrication and culture

Three-dimensional engineered muscle tissues (myobundles) were formed as described previously (Supplementary Figure 1) (Khodabukus et al., 2019). Briefly, laser-cut Cerex frames were placed in polydimethylsiloxane (PDMS) molds containing two semicylindrical wells (7 mm long, 2 mm diameter). The cell/hydrogel solution was made by mixing a cell solution (per myobundle,  $7.5 \times 10^5$  cells in 17.2 µl media + 2 µl of 50 U/ml thrombin in 0.1% BSA in PBS) and an ice-cold hydrogel solution (11 µl media + 10 µl Matrigel + 10 µl of 20 mg/ml fibrinogen in DMEM) and was poured in the PDMS molds and left to gel for 45 min to generate myobundles. Myobundles were dynamically cultured on a rocker for 4 days in growth media supplemented with

1.5 mg/ml 6-aminocaproic acid (ACA, Sigma, A7824). Media was then switched to serum-free differentiation media (DM) consisting of low-glucose DMEM, 1% N2-supplement (ThermoFisher, 17502048), 100 U/ml penicillin (Sigma, P7794), and 2 mg/ml ACA, with media changed daily (Rao et al., 2018).

### Notexin-induced injury and pharmacological treatment of myobundles

After 1 week of differentiation, myobundles were exposed to a single dose (1 or 3  $\mu$ g/ml) of Notexin (NTX) for 6 h and DM was then collected every 24 h and fully replaced with fresh media. Alternatively, myobundles differentiated for 1 week were treated daily with fresh DM containing 10 or 100 nM cerivastatin (Cayman chemical, 20362), 50 or 250 nM pravastatin (Cayman chemical, 10010342), 100 or 500 ng/ml IGF-1 (Prospecbio, CYT-216), or 1 or 25  $\mu$ M dexamethasone. Cerivastatin, pravastatin, and dexamethasone were initially reconstituted to 10 mM in DMSO and IGF-1 was reconstituted to 1 mg/ml in 0.1% bovine serum albumin (BSA) in PBS. Appropriate amounts of DMSO and 0.1% BSA were added to culture media to ensure the same vehicle concentration in each experimental group. All concentrations were chosen to be physiologically relevant and within reported ranges of Cmax values in human serum for cerivastatin (Muck et al., 1998, 2000), pravastatin (Corsini et al., 1999; Escobar et al., 2005), IGF-1 (Rabkin et al., 1996; Thankamony et al., 2014), and dexamethasone (Queckenberg et al., 2011; Spoorenberg et al., 2014). All drugs were applied fresh every 24 h with a complete media change. Culture media samples were collected every 24 h to measure biomarker released by myobundles in response to pharmacological treatment, whereas histological and functional characterization were conducted after 7 days treatment unless stated otherwise.

### Immunohistochemistry

Fixation and sectioning of myobundles were performed as described previously (Khodabukus et al., 2019). Cross-sections were stained with  $\beta$ -spectrin (Abcam, ab2808), dystrophin (Abcam, ab15277), or sarcomeric alpha-actinin (Sigma, A7811) at a 1:200 dilution in blocking solution for 45 min at room temperature. After washing samples with PBS 3 times, they were incubated with secondary antibodies, including Hoescht 33342 (ThermoFisher, H3570) and Alexa Fluor conjugated Phalloidin (ThermoFisher, A12381), at 1:400 dilution in blocking solution for 45 min. Immunofluorescence images were acquired using a Leica SP5 inverted confocal microscope and analyzed using ImageJ.

### Measurement of myobundle contractile function

Electrically stimulated contractile force generation of myobundles was measured using a custom force measurement setup as described previously (Khodabukus et al., 2019). Briefly, single myobundles were transferred to the bath of a custom-made force measurement setup, maintained at 37°C, and stretched to 112% of their resting length via a computer-controlled motorized linear actuator. Ninety V/cm, 5-ms electrical pulse was applied using a pair of platinum electrodes and the twitch force was recorded. At 12% stretch, 1-s-long stimulation trains at 5, 10, and 20 Hz (tetanus) frequency were applied and the contractile force was recorded to determine the force-frequency relationship. Contractile force traces were analyzed for peak twitch or tetanus force using a custom MATLAB program.

### Myobundle-secreted protein expression

sTnI, FABP3, Myl3, and cTnT protein amounts were quantified in media samples using the Meso Scale Discovery (MSD, Rockville, Maryland) Muscle Injury Panel 1 reagent kit (MSD, K15181C). CKm was measured using the MSD Muscle Injury Panel 2 reagent kit (MSD, K15180C). Matrix metalloproteinase (MMP)-1 and MMP-3 were quantified using MSD Human MMP 3-Plex kit (MSD, K151034C). MMP-2 was quantified using MSD Human MMP 2-Plex kit (MSD, K151033C). CK activity was measured by standard clinical chemistry techniques on the Siemens Advia 2400 platform. All assays were performed as per the manufacturer's instructions. Samples were stored at -80°C prior to analysis and assayed without dilution except for CKm which was diluted 1:15.

### Statistical analysis

All data are presented as mean  $\pm$  SEM. Statistical analysis was conducted by one-way ANOVA followed by post hoc Tukey's t test or two-way ANOVA followed by post hoc Dunnett t test.

## RESULTS

### Effect of Notexin on Myobundle Structure

We first assessed if human myobundles can be used to detect muscle injury by applying 0 (CTL), 1, or 3  $\mu$ g/ml of notexin (NTX), a neurotoxic phospholipase isolated from the Australian tiger snake, known to induce severe muscle injury (Dixon and Harris, 1996). Without injury (0  $\mu$ g/ml NTX), myobundle cross-sections contained  $591 \pm 34$  nuclei and  $0.27 \pm 0.02$  mm<sup>2</sup> of area positive for f-actin (corresponding to muscle mass [Madden et al., 2015]), which 6 days after NTX application were found to be reduced in average by 25% (Figs. 1A and 1B) and 30% (Figs. 1C and 1D), respectively, demonstrating that the toxin induced significant muscle death and injury. Furthermore, myotube diameter (CTL:  $15.47 \pm 0.26$   $\mu$ m) was also reduced in average by 10% and 15% at 1 and 3  $\mu$ g/ml NTX, respectively (Figs. 1E and 1F).

### Effect of Notexin on Biomarker Release

We next assessed cumulative levels of biomarkers released by the myobundles into the culture media over a 7-day period post-injury. The release of the traditional non-tissue-specific biomarkers CK (Figs. 2A and 2B) and LDH (Figs. 2C and 2D) into the culture media were significantly increased following NTX injury. Out of four members of MIP, three (sTnI, Fabp3, and CKm) could be detected in the culture media, whereas Myl3 release was below the detection limit of 10 ng/ml (data not shown). We also found that cardiac troponin T (cTnT) could be readily detected in the culture media and analyzed cTnT release in all subsequent studies. The three detectable MIP biomarkers and cTnT were all significantly increased following NTX injury (Figs. 2E-L). CK, LDH, CKm, and cTnT also showed a dose-dependent increase in cumulative release from 1 to 3  $\mu$ g/ml NTX. Maximal release occurred within the first 2-3 days following injury when maximal damage by NTX would be expected to occur. Overall, the clearly detectable response to NTX in myobundles suggested that this human tissue-engineered system could serve as an in vitro platform to study the biomarker release in response to injury or myopathic changes.

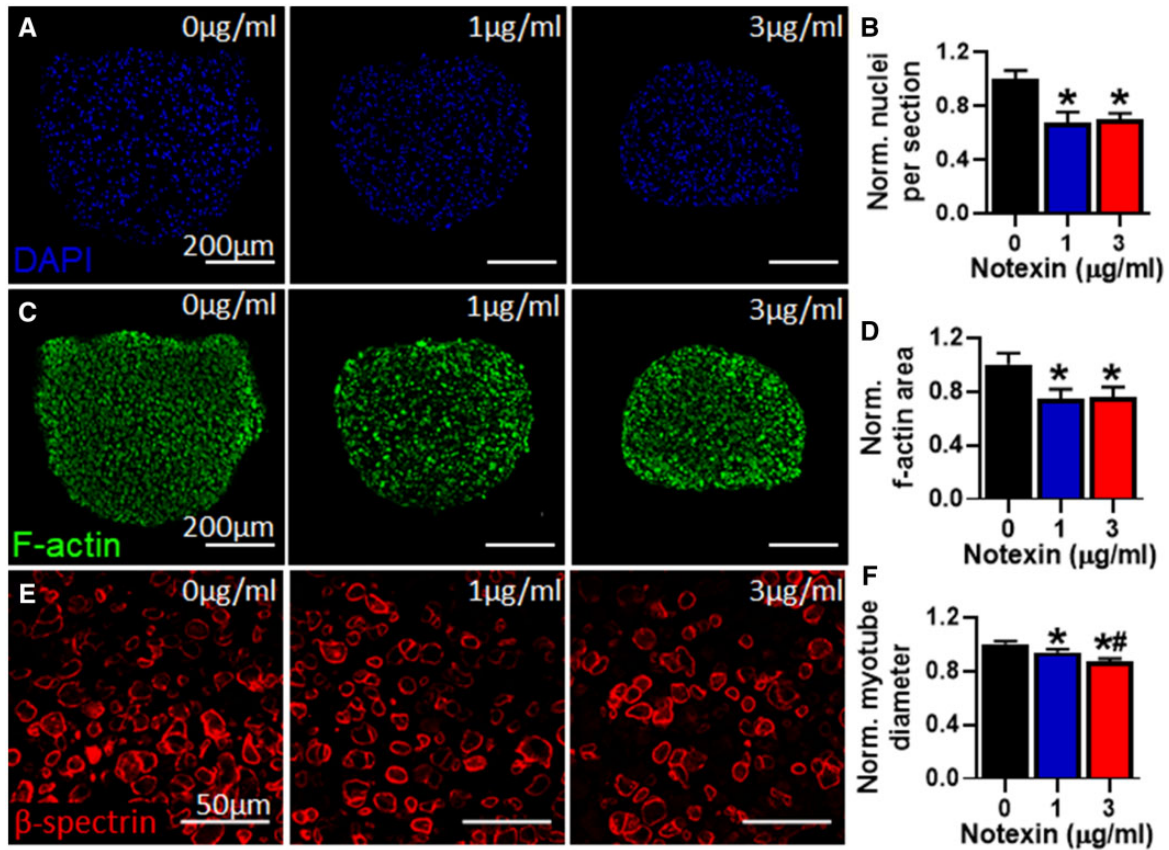


**Figure 1.** Effects of notexin injury on myobundle structure. A, Representative myobundle cross-sectional images stained for nuclei (DAPI). B, Quantification of nuclei number per myobundle cross-section normalized to drug-free control ( $n = 4$  myobundles per group,  $n = 2$  technical replicates from  $N = 1$  donor). C, Representative myobundle cross-sectional images stained for filamentous actin (f-actin). D, Quantification of F-actin positive area per myobundle cross-section normalized to drug-free control ( $n = 4$  myobundles per group from  $N = 1$  donor). E, Representative myobundle cross-sectional images stained for  $\beta$ -spectrin. F, Quantification of myotube diameter relative to drug-free control ( $n = 100$  myotubes from 4 myobundles per group from  $N = 1$  donor). \* $p < .01$  from 0  $\mu\text{g/ml}$  notexin and \*\* $p < .01$  from 1  $\mu\text{g/ml}$  notexin.

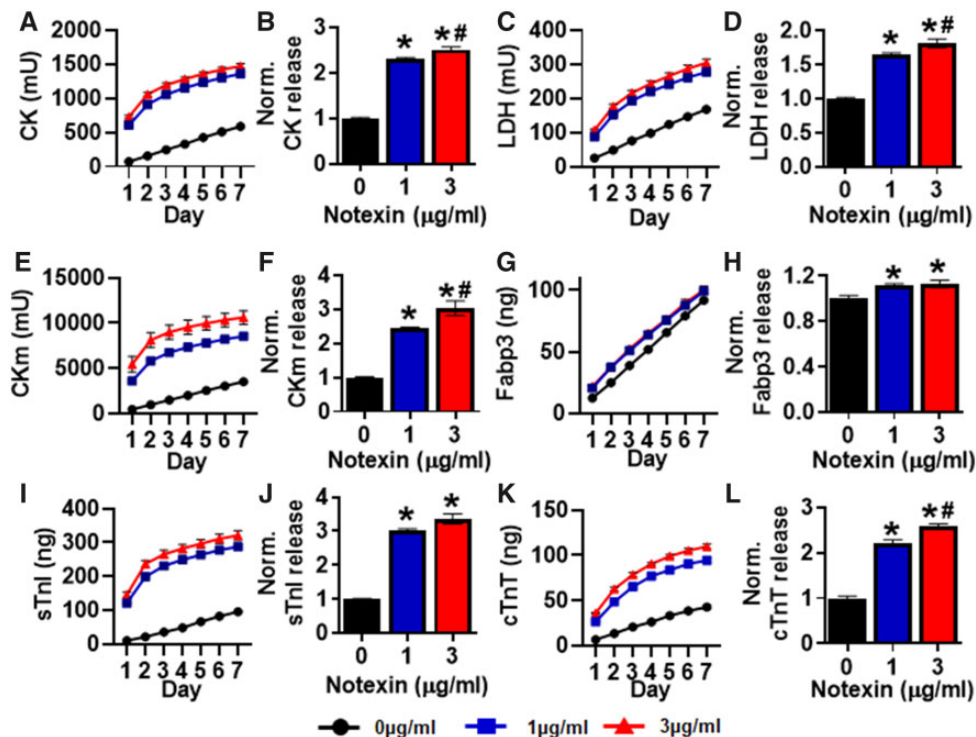


**Figure 2.** Effects of notexin injury on myobundle biomarker release. Cumulative biomarker release profiles and quantifications of total release during 7 days normalized to drug-free control after NTX injury shown for (A, B) CK, (C, D) LDH, (E, F) CKm, (G, H) Fabp3, (I, J) sTnI, and (K, L) cTnT. Quantifications performed from  $n = 4$  myobundles per donor,  $n = 2$  technical replicates from  $N = 1$  donor. \* $p < .01$  from 0  $\mu\text{g/ml}$  notexin and \*\* $p < .05$  from 1  $\mu\text{g/ml}$  notexin.

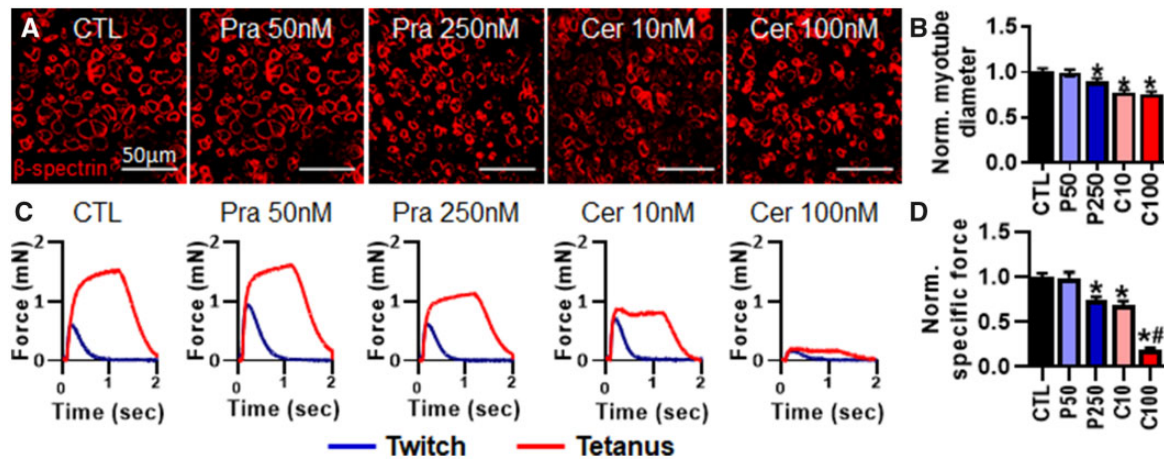


**Figure 3.** Effects of 7-day application of pravastatin and cerivastatin on myotube diameter and contractile function. A, Representative images of myobundle cross-sections stained for  $\beta$ -spectrin. B, Quantification of myotube diameter from  $\beta$ -spectrin stainings normalized to drug-free control ( $n = 200$  myotubes from 8 myobundles per group from  $N = 2$  donors). C, Representative force traces during twitch and tetanic contraction. D, Quantification of specific force during tetanic contraction normalized to drug-free control ( $n = 8$  myobundles,  $n = 1$  technical replicate, from  $N = 2$  donors). \* $p < .01$  from CTL and # $p < .001$  from C10. CTL, drug-free control; P50, 250 nM pravastatin; P250, 250 nM pravastatin; C10, 10 nM cerivastatin; C100, 100 nM cerivastatin.

### Effect of Pravastatin and Cerivastatin on Myotube Structure and Function

To continue to evaluate suitability of the human myobundle system for toxicity testing, we measured myobundle function and biomarker release in response to application of two statins with variable levels of myotoxicity. Specifically, myobundles were treated for 7 days with physiologically relevant concentrations of the clinically approved pravastatin (50 or 250 nM) or the clinically withdrawn cerivastatin (10 or 100 nM). Following 1-week statin treatment, we found that myotube diameter (CTL:  $15.19 \pm 0.37 \mu\text{m}$ ) was significantly reduced in average by 23% and 25% with 10 and 100 nM cerivastatin treatment, respectively (Figs. 3A and 3B). Generated specific force (CTL:  $6.17 \pm 0.77 \text{ mN/mm}^2$ ) was significantly decreased by 26% with 250 nM pravastatin treatment (Figs. 3C and 3D), whereas 10 and 100 nM cerivastatin treatment resulted in 36% and 85% decrease in specific force, respectively (Figs. 3C and 3D). Overall, the greater decrease in myotube diameter and contractile function demonstrated that cerivastatin induced greater myotoxicity than pravastatin.

### Effect of Pravastatin and Cerivastatin on Biomarker Release

We next evaluated the effect of pravastatin and cerivastatin on cumulative biomarker release over the 7-day treatment period. Cerivastatin but not pravastatin induced significant dose-dependent increase in the traditional injury biomarkers CK (Figs. 4A and 4B) and LDH (Figs. 4C and 4D). Similar to the traditional injury biomarkers, cerivastatin but not pravastatin induced significant increases in MIP biomarker and cTnT release (Figs. 4E–L). Interestingly, we found dose-dependent increases in CKm and sTnI release but not Fabp3 and cTnT with cerivastatin treatment. Overall, cerivastatin increased biomarker release that correlated with changes in myobundle structure and function, whereas biomarker release with pravastatin treatment did not significantly change despite the observed decrease in specific force generation at highest tested dose.

### Effect of IGF-1 and Dexamethasone on Myotube Diameter and Myobundle Function

We next assessed the effect of the hypertrophic agent IGF-1 (Adams and Haddad, 1996; Jacquemin et al., 2004; Rommel et al., 2001) and atrophic agent dexamethasone (Shimizu et al., 2011; Waddell et al., 2008) on myotube size, myobundle function, and biomarker release. The 7-day treatment with 0.1 and 0.5 mg/ml IGF-1 significantly increased myotube diameter (CTL:  $12.49 \pm 0.17 \mu\text{m}$ ) by 26% and 21% in average, respectively (Figs. 5A and 5B). In contrast, 1 and 25  $\mu\text{M}$  dexamethasone significantly reduced myotube diameter by 14% and 12%, respectively (Figs. 5A and 5B). Although IGF-1 treatment had an apparent trend but no statistically significant effect on specific force, 1 and 25  $\mu\text{M}$  dexamethasone significantly decreased specific force by 56% and 67%, respectively, compared with drug-free myobundles (CTL:  $6.67 \pm 1.06 \text{ mN/mm}^2$ ) (Figs. 5C and 5D).

### Effect of IGF-1 and Dexamethasone on Biomarker Release

We next evaluated the effect of IGF-1 and dexamethasone treatment on traditional and MIP biomarker release during 7-day treatment period. Both 0.1 and 0.5 mg/ml IGF-1 treatment significantly increased levels of the traditional biomarkers CK (Figs. 6A and 6B) and LDH (Figs. 6C and 6D). In contrast, levels of both CK and LDH dropped below the lower limit of detection within the first 24 h of 1 and 25  $\mu\text{M}$  dexamethasone treatment. Both 0.1 and 0.5 mg/ml IGF-1 treatment also significantly increased cumulative levels of CKm (Figs. 6E and 6F), sTnI (Figs. 6I and 6J), and cTnT (Figs. 6K and 6L) but not Fabp3 (Figs. 6G and 6H). In contrast, both 1 and 25  $\mu\text{M}$  dexamethasone significantly decreased cumulative levels of CKm, Fabp3, sTnI, and cTnT.

### Effect of IGF-1 and Dexamethasone on Myobundle Morphology and MMP Release

Due to unexpected changes in contractile function and biomarker release, we additionally assessed changes in myobundle morphology during application of IGF-1 and dexamethasone. Interestingly, with 7-day dexamethasone application, number of nuclei and f-actin positive area per cross-section were

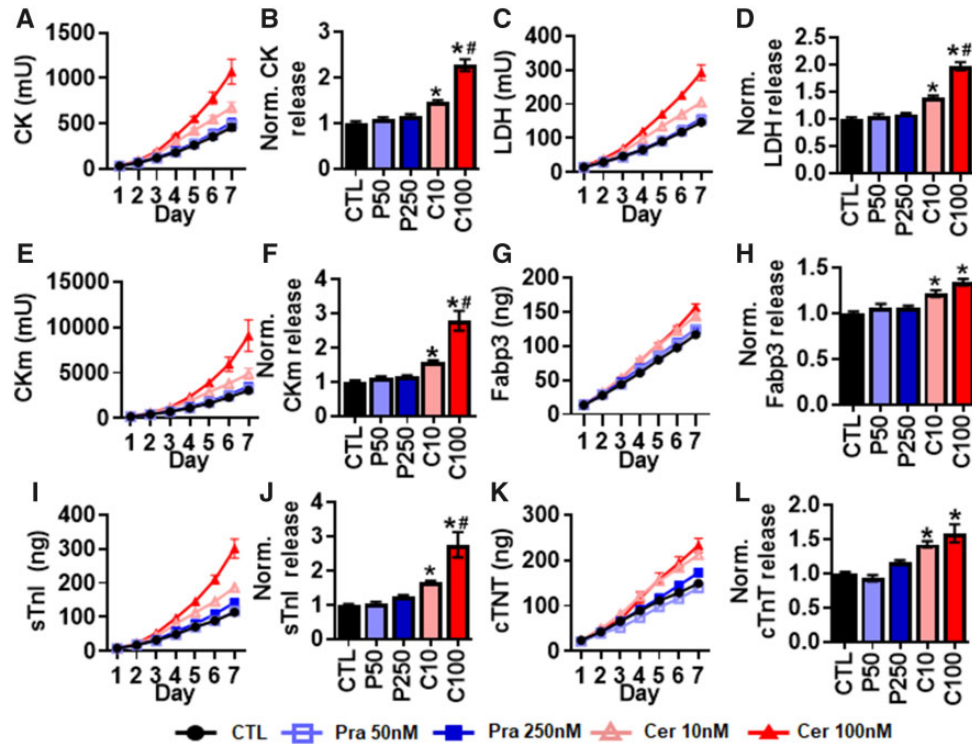


**Figure 4.** Effects of 7-day pravastatin and cerivastatin application on myobundle biomarker release. Cumulative biomarker release profiles and quantifications of total release normalized to drug-free control during 7 days of pravastatin or cerivastatin application, shown for (A, B) CK, (C, D) LDH, (E, F) CKm, (G, H) Fabp3, (I, J) sTnI, and (K, L) cTnT. Quantifications performed from  $n=8$  myobundles per donor,  $n=2$  technical replicates from  $N=2$  donors. \* $p < .01$  from CTL and # $p < .05$  from C10. CTL, drug-free control; P50, 250 nM pravastatin; P250, 250 nM pravastatin; C10, 10 nM cerivastatin; C100, 100 nM cerivastatin.

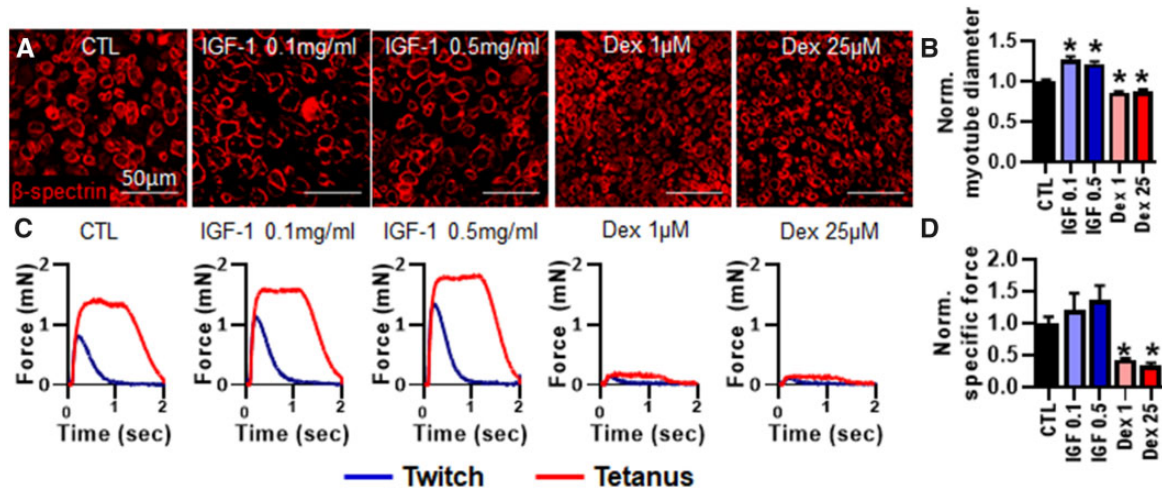


**Figure 5.** Effects of 7-day IGF-1 and dexamethasone treatment on myotube diameter and contractile function. A, Representative images of myobundle cross-sections stained for  $\beta$ -spectrin. B, Quantification of myotube diameter from  $\beta$ -spectrin stainings normalized to drug-free control ( $n=200$  myotubes from 8 myobundles per group from  $N=2$  donors). C, Representative force traces during twitch and tetanic contraction. D, Quantification of specific force during tetanic contraction normalized to drug-free control ( $n=8$  myobundles from  $N=2$  donors). \* $p < .01$  from CTL. CTL, drug-free control. IGF 0.1, 0.1 mg/ml IGF-1; IGF 0.5, 0.5 mg/ml IGF-1; Dex 1, 1  $\mu$ M dexamethasone; Dex 25, 25  $\mu$ M dexamethasone.

decreased in average by 18% (Figs. 7A and 7B) and 60% (Figs. 7C and 7D), respectively, compared with control values (CTL:  $541 \pm 37$  nuclei and  $0.24 \pm 0.02$  mm<sup>2</sup>). Due to this large decrease in myobundle cross-sectional area, we assessed the secretion of MMP-1, -2, and -3 that regulate extracellular matrix remodeling (Chen and Li, 2009; Stamenkovic, 2003) at highest drug doses. We found that 0.5 mg/ml IGF-1 and 25  $\mu$ M dexamethasone

applications significantly decreased the 7-day average cumulative levels of MMP-1 by 43% and 81%, respectively (Figs. 7E and 7F). On the other hand, 25  $\mu$ M dexamethasone application increased the average 7-day cumulative levels of MMP-2 (Figs. 7G and 7H) and MMP-3 (Figs. 7I and 7J) by 1.9 and 7.2-fold, respectively, whereas 0.5 mg/ml IGF-1 showed no significant effect on MMP-2 or MMP-3 release.

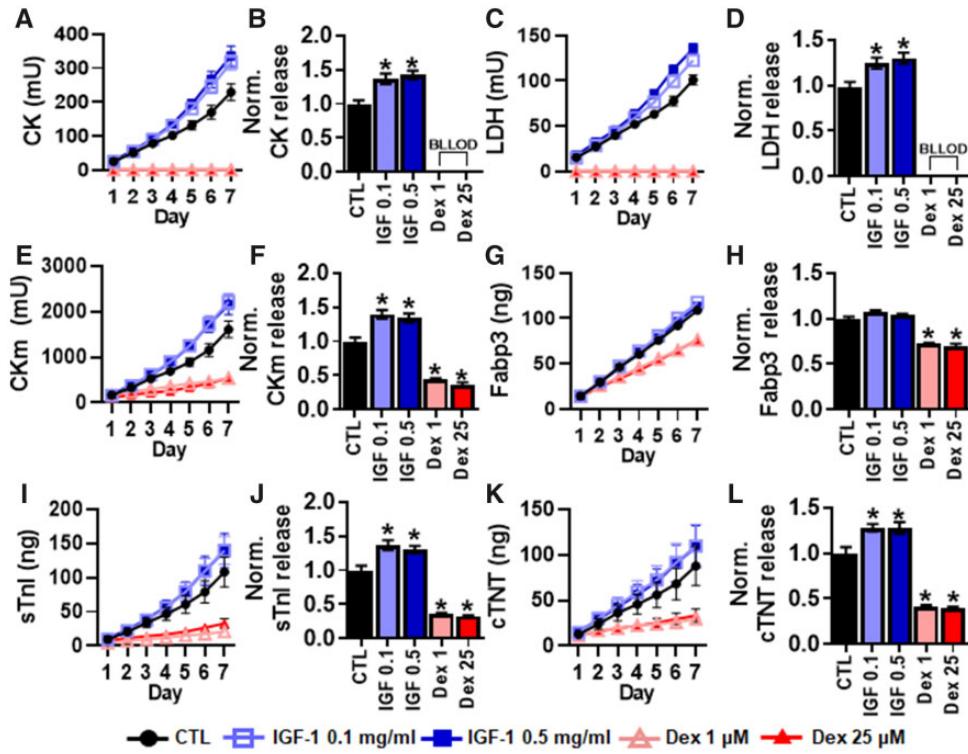


**Figure 6.** Effects of 7-day IGF-1 and dexamethasone application on myobundle biomarker release. Cumulative biomarker release profiles and quantifications of total release normalized to drug-free control during 7 days of IGF-1 and dexamethasone application, shown for (A, B) CK, (C, D) LDH, (E, F) CKm, (G, H) Fabp3, (I, J) sTnI, and (K, L) cTnT release after 7 days. \**p* < .01 from CTL. Quantifications performed from *n* = 8 myobundles per donor, *n* = 2 technical replicate, from *N* = 2 donors. CTL, drug-free control; IGF 0.1, 0.1 mg/ml IGF-1; IGF 0.5, 0.5 mg/ml IGF-1; Dex 1, 1 μM dexamethasone; Dex 25, 25 μM dexamethasone; BLOOD, below lower limit of detection.

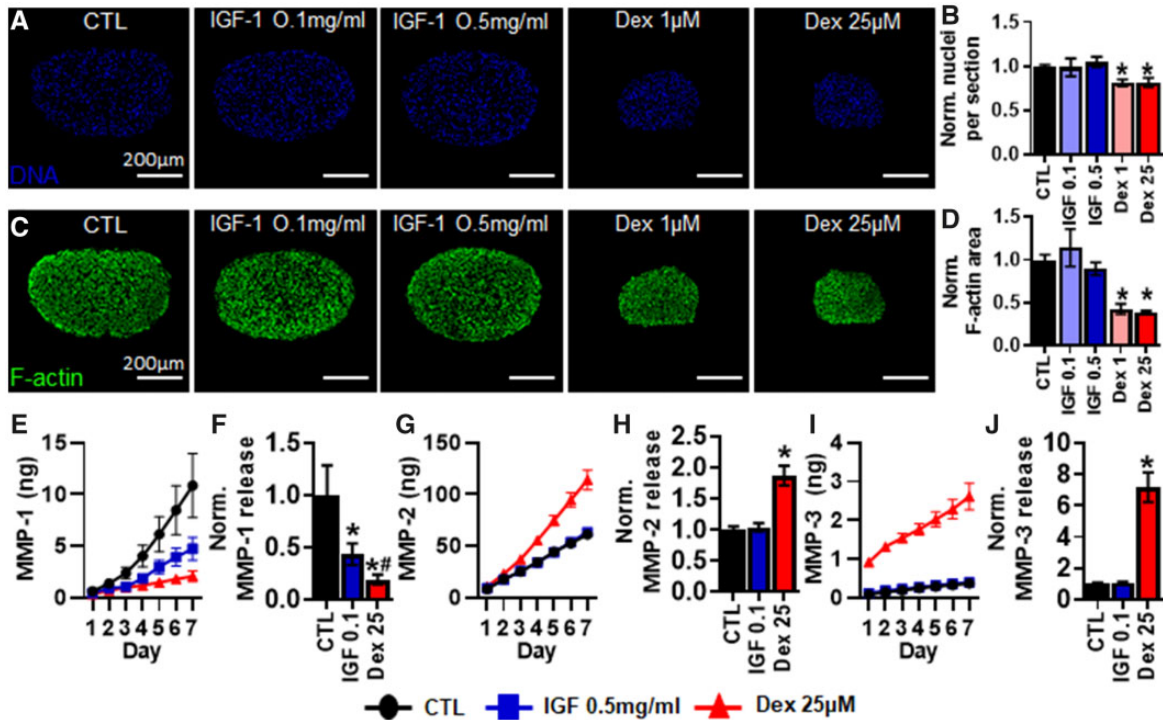


**Figure 7.** Effects of 7-day pravastatin and cerivastatin application on myobundle morphology and MMP release. A, Representative myobundle cross-sectional images stained for nuclei (DAPI). B, Quantification of nuclei number per myobundle cross-section normalized to drug-free control (*n* = 200 myotubes from 8 myobundles per group, from *N* = 2 donors). C, Representative myobundle cross-sectional images stained for filamentous actin (F-actin). D, Quantification of f-actin area per myobundle cross-section normalized to drug-free controls (*n* = 8 myobundles from *N* = 2 donors). Cumulative daily release profile and 7-day cumulative quantification of (E, F) MMP-1, (G, H) MMP-2, (I, J) MMP-3 (*n* = 8 myobundles, *n* = 2 technical replicates from *N* = 2 donors). \**p* < .01 from CTL and #*p* < .05 from IGF 0.5. CTL, drug-free control; IGF 0.1, 0.1 mg/ml IGF-1; IGF 0.5, 0.5 mg/ml IGF-1; Dex 1, 1 μM dexamethasone; Dex 25, 25 μM dexamethasone.

## DISCUSSION

In this study, we utilized the primary human myobundle system to assess the structural, functional, and biomarker responses to a set of myotoxic compounds and natural hormones. Specifically, we assessed the release of both classical and novel MIP biomarkers in response to acute (6-h) application of the snake venom notexin and chronic (7-day) application of the pharmacological toxicants, cerivastatin and dexamethasone, and their respectively related nontoxicants, pravastatin and IGF-1. We found expected myobundle injury responses to notexin and statins; however, despite observing the decreased contractile function by both cerivastatin and dexamethasone, their respective biomarker release profiles had opposite trends with dexamethasone treatment showing significantly decreased or undetectable biomarker levels. However, we found that culture media levels of MMP-2 and -3 were increased in this case, suggesting that MMPs could be potentially used to assess glucocorticoid-induced toxicity in preclinical and clinical studies. Together, this proof-of-concept study shows that human myobundle system could be used as a testbed for evaluation of known and discovery of new biomarkers for skeletal muscle disorders.

In all conditions tested, our analysis of myobundle-secreted media detected the presence of 3 out of the 4 MIP biomarkers, with Myl3 falling below the level of detection. Myl3 is the mature isoform of slow myosin light chain expressed in late fetal (>31 weeks) and adult human skeletal muscle (Butler-Browne et al., 1990; Pons et al., 1987) and, along with other 3 MIP biomarkers, is detected in healthy human serum and elevated in DMD patients (Burch et al., 2015; Goldstein, 2017). We previously showed that the contractile function and myosin heavy chain expression of myobundles were similar to those of fetal human skeletal muscle (Madden et al., 2015; Rao et al., 2018). Thus, our inability to detect Myl3 most likely reflected the relatively immature phenotype of myobundles. Similarly, our ability to detect cTnT, which is highly expressed in developing, regenerating, or denervated skeletal muscle (Bodor et al., 1997) may reflect particular properties of the myobundle system. On the other hand, cTnT is also expressed in a subset of healthy adult skeletal muscles (Bodor et al., 1997) and found to increase with muscle denervation (Xu et al., 2017) and in patients with neuromuscular diseases independent of cardiac involvement (Rittoo et al., 2014). Taken together, cTnT could have utility as a biomarker for skeletal muscle disorders, though it must be used in conjunction with other biomarkers to exclude potential confounding effects from cardiac muscle. Besides assessing muscle damage, cTnT and Myl3 could serve as markers of advanced skeletal muscle maturation, necessary for clinical predictability of in vitro systems in drug development applications. Importantly, measured biomarker release will need to be carefully interpreted for treatments that promote muscle differentiation or hypertrophy. In our study, IGF-I treatment increased biomarker release (Figure 6) without significantly changing myobundle function (Figs. 5C and 5D), most likely due to stimulated muscle hypertrophy (Figs. 5A and 5B) and/or differentiation (Delaporte et al., 1986; Musaro and Rosenthal, 1999). Biomarker normalization is a common issue in the field due to the lack of known secreted factors that correlate to cell size or protein content (Gunasekaran et al., 2019). However, by combining biomarker, morphological, and functional measurements in myobundles, the cause and impact of biomarker release changes can be more accurately assessed.

In the present study, the release profile of both the classical and MIP biomarkers replicated those reported in preclinical animal models in response to large-scale notexin injury (Sharp et al., 1993) and cerivastatin (Burch et al., 2016) treatment. Furthermore, this increase in biomarker release correlated with a measured loss of muscle function. In cerivastatin-treated myobundles, we observed a 200%–300% increase in sTnI and CKm levels and only a 20%–30% increase in Fabp3 (Figure 4). This decrease in dynamic range of Fabp3 is in agreement with measurements in human subjects, where DMD patients showed an 8-fold increase in Fabp3 versus 20–30-fold increase in sTnI and CKm (Burch et al., 2015). Furthermore, preclinical and clinical studies have suggested that the MIP biomarkers have increased sensitivity and specificity to muscle injury in comparison to traditional biomarkers (Burch et al., 2016; Goldstein, 2017). Consistent with this notion, traditional biomarkers in our myobundle studies were below the lower limit of detection during application of dexamethasone (Figs. 6A–D), whereas the MIP biomarkers were still detectable (Figs. 6E–J). However, in notexin and statin studies we found comparable sensitivities between the traditional and MIP biomarkers (Figs. 2 and 4), potentially due to the myobundle immature phenotype or the presence of only myogenic cells and fibroblasts.

Interestingly, we also found that notexin, cerivastatin, and dexamethasone all decreased contractile function, but while notexin and cerivastatin increased release of traditional and MIP biomarkers, dexamethasone had the opposite effects on biomarker release. The effect of dexamethasone on circulating CK and LDH levels in human and rodent in vivo studies are conflicting, with reports of increased (Lee et al., 2018; Orzechowski et al., 2002; Song et al., 2018), decreased (Khaleeli et al., 1983; Kim et al., 2015; Rajashree and Puvanakrishnan, 1998), or non-detectable (Minetto et al., 2010) levels in blood. Our inability to detect secreted CK and LDH with dexamethasone treatment of myobundles could be related to their lack of innervation-induced contractile activity known to decrease circulating CK levels (Rochkind and Shainberg, 2017; Sayers et al., 2000) and skeletal muscle CK transcript levels (Washabaugh et al., 2001). Furthermore, denervation was shown to render muscles more vulnerable to atrophy and functional loss from dexamethasone treatment (Mozaffar et al., 2007; Rouleau et al., 1987). In myobundles, dexamethasone also significantly decreased myotube diameter as has been reported in skeletal muscle tissues engineered from the mouse C2C12 cell line (Shimizu et al., 2017) and attributed to decreased activation of the anabolic Akt/mTOR signaling pathway (Schakman et al., 2013; Shimizu et al., 2011) and increased catabolism by proteasomal activation and induction of the atrogenes (Castillero et al., 2013; Waddell et al., 2008). Together, this suggests that the mode of injury determines both classical and MIP biomarker profile, with interventions that induce significant necrosis, such as notexin (Sharp et al., 1993) and cerivastatin (Westwood et al., 2005), increasing biomarker release. On the other hand, dexamethasone reduced biomarker release while inducing significant ECM remodeling and myobundle compaction (Figs. 7C and 7D), which would not have been easily detected in traditional 2D cultures. Following up on this observation, we identified MMP-2 and -3 as potential biomarkers of glucocorticoid action, highlighting the prospective utility of the myobundle model for studying and identifying novel biomarkers. In agreement with our findings, elevated circulating levels of MMP-3 have been identified in DMD patients treated with glucocorticoids (Hathout et al., 2016a).



The ability to model and study glucocorticoid-induced muscle atrophy in a human system is essential given the importance of glucocorticoids for treating DMD and their adverse side effects (Bushby et al., 2010; Quattrocelli et al., 2017). As an in vitro surrogate for human skeletal muscle, the myobundle system could be used in the future to rapidly screen and identify novel biomarkers for muscle atrophy (such as *serpina3n* [Gueugneau et al., 2018]) using proteomic (Ayoglu et al., 2014; Hathout et al., 2015) and microRNA (Si et al., 2018; Siracusa et al., 2018) profiling of culture media. Moreover, myobundles could serve to screen novel glucocorticoids with potentially lower side effects (Conklin et al., 2018), identify novel adjunctive therapies (Jesinkey et al., 2014), and optimize glucocorticoid dosing regimens (Quattrocelli et al., 2017) to improve patient safety and therapeutic outcomes. Of further importance is that in agreement with clinical (Maji et al., 2013; Meor Anuar Shuhaili et al., 2017) and cell culture (Cafforio et al., 2005; Kaufmann et al., 2006) studies, myotoxicity in myobundles was significantly higher for cerivastatin than either lovastatin or pravastatin (Madden et al., 2015; Zhang et al., 2018). Therefore the primary human myobundles could also serve to predict myotoxicity of next-generation statins, identify novel adjunctive therapies to mitigate muscle damage, and study the mechanisms of statin-induced toxicity (Zhang et al., 2018) by correlating biomarker release of myobundles to changes in their contractile function, stiffness, metabolism (Davis et al., 2017; Khodabukus et al., 2019), and/or ECM composition (Hinds et al., 2011). Interestingly, we found that high doses of pravastatin and low doses of cerivastatin induced similar functional and morphological changes in myobundles, but biomarker release was only increased with cerivastatin. Although this discrepancy could be due to donor variability, it may point to different myotoxic mechanisms between pravastatin and cerivastatin via distinct effects on mitochondrial toxicity (Kaufmann et al., 2006), ROS generation (Chen et al., 2016), MAFbx expression (Bonifacio et al., 2015), autophagy (Chen et al., 2016), and Akt signaling (Bonifacio et al., 2015; Godoy et al., 2019).

Improving the utility of myobundle system for drug discovery would necessitate the development of methods to increase tissue maturity by use of select hormones (Butler-Browne et al., 1990; Hamalainen and Pette, 1997), small molecules (Bian and Bursac, 2012; Selvaraj et al., 2019), motor neuron co-culture (Afshar Bakooshli et al., 2019; Larkin et al., 2006), and electrical (Khodabukus et al., 2019) or mechanical (Khodabukus et al., 2019; Powell et al., 2002; Rangarajan et al., 2014) stimulation. Incorporation of additional muscle-resident cell types within myobundles, such as immune (Juhás et al., 2018), vascular (Bersini et al., 2018; Gholobova et al., 2015), and neuronal (Afshar Bakooshli et al., 2019; Osaki et al., 2018; Vila et al., 2019) cells would better model native muscle composition, function, and regenerative potential. In support, the incorporation of bone marrow derived macrophages into adult rat myobundles was required for a biomimetic regenerative response to cardiotoxin-induced injury (Juhás et al., 2018). Additionally, the ability to predict clinical drug toxicity and identify tissue-specific biomarkers would benefit from use of “human-on-a-chip” models whereby myobundles would be directly coupled to cardiac, liver, kidney, gut, adipose, and other human organoids to better model drug metabolism, biodistribution, and complex organ-organ interactions (Oleaga et al., 2016; Skardal et al., 2017; Wang et al., 2019). Furthermore, performing high-throughput drug screening for large numbers of patients will require significant miniaturization of engineered muscle size (Afshar Bakooshli et al., 2019; Mills et al., 2019; Vandenburg et al., 2008), the incorporation of

automation compatible tissue fabrication, and functional testing modalities, such as micro pillar deflection (Mills et al., 2019; Vandenburg et al., 2008), cantilever (Oleaga et al., 2016), or alternative displacement measurement systems (Zhang et al., 2018).

In summary, our studies demonstrate the potential utility of the human primary myobundle platform for assessing drug toxicity in human skeletal muscle, evaluating the expression of prospective muscle biomarkers identified in preclinical animal models, and identifying new biomarkers for skeletal muscle injury and disease.

## SUPPLEMENTARY DATA

Supplementary data are available at *Toxicological Sciences* online.

## FUNDING

National Institute of Arthritis and Musculoskeletal and Skin Disease (NIAMS) (NIH Grant Nos. AR070543, AR065873); National Institute on Aging (NIA) (AG054840); NIH Common Fund for the Microphysiological Systems Initiative and NIAMS (UH3TR000505, UG3TR002142, U01EB028901); and a research collaboration agreement with Pfizer. The content of the manuscript is solely the responsibility of the authors and does not necessarily represent the official views of the funding agencies.

## DECLARATION OF CONFLICTING INTERESTS

R.G. and V.S.V. are employees of Pfizer Inc.

## REFERENCES

- Adams, G. R., and Haddad, F. (1996). The relationships among igf-1, DNA content, and protein accumulation during skeletal muscle hypertrophy. *J. Appl. Physiol.* **81**, 2509–2516.
- Afshar Bakooshli, M., Lippmann, E. S., Mulcahy, B., Iyer, N., Nguyen, C. T., Tung, K., Stewart, B. A., van den Dorpel, H., Fuehrmann, T., Shoichet, M., et al. (2019). A 3d culture model of innervated human skeletal muscle enables studies of the adult neuromuscular junction. *Elife* **8**, e44530.
- Ayoglu, B., Chaouch, A., Lochmuller, H., Politano, L., Bertini, E., Spitali, P., Hiller, M., Niks, E. H., Gualandi, F., Ponten, F., et al. (2014). Affinity proteomics within rare diseases: A bio-nmd study for blood biomarkers of muscular dystrophies. *EMBO Mol. Med.* **6**, 918–936.
- Bersini, S., Gilardi, M., Ugolini, G. S., Sansoni, V., Talo, G., Peregó, S., Zanotti, S., Ostano, P., Mora, M., Soncini, M., et al. (2018). Engineering an environment for the study of fibrosis: A 3d human muscle model with endothelium specificity and endomysium. *Cell Rep.* **25**, 3858–3868. e3854.
- Bian, W., and Bursac, N. (2012). Soluble miniagrin enhances contractile function of engineered skeletal muscle. *FASEB J.* **26**, 955–965.
- Bodie, K., Buck, W. R., Pieh, J., Liguori, M. J., and Popp, A. (2016). Biomarker evaluation of skeletal muscle toxicity following clofibrate administration in rats. *Exp. Toxicol. Pathol.* **68**, 289–299.
- Bodor, G. S., Survant, L., Voss, E. M., Smith, S., Porterfield, D., and Apple, F. S. (1997). Cardiac troponin t composition in normal and regenerating human skeletal muscle. *Clin. Chem.* **43**, 476–484.

- Bonifacio, A., Sanvee, G. M., Bouitbir, J., and Krahenbuhl, S. (2015). The akt/mTOR signaling pathway plays a key role in statin-induced myotoxicity. *Biochim. Biophys. Acta* **1853**, 1841–1849.
- Broer, T., Khodabukus, A., and Bursac, N. (2020). Can we mimic skeletal muscles for novel drug discovery? *Expert Opin. Drug Discov.* **1–3**. doi:10.1080/17460441.2020.1736031
- Burch, P. M., Greg Hall, D., Walker, E. G., Bracken, W., Giovanelli, R., Goldstein, R., Higgs, R. E., King, N. M., Lane, P., Sauer, J. M., et al. (2016). Evaluation of the relative performance of drug-induced skeletal muscle injury biomarkers in rats. *Toxicol. Sci.* **150**, 247–256.
- Burch, P. M., Pogoryelova, O., Goldstein, R., Bennett, D., Guglieri, M., Straub, V., Bushby, K., Lochmuller, H., and Morris, C. (2015). Muscle-derived proteins as serum biomarkers for monitoring disease progression in three forms of muscular dystrophy. *J. Neuromuscul. Dis.* **2**, 241–255.
- Bushby, K., Finkel, R., Birnkrant, D. J., Case, L. E., Clemens, P. R., Cripe, L., Kaul, A., Kinnett, K., McDonald, C., Pandya, S., et al. (2010). Diagnosis and management of Duchenne muscular dystrophy, part 1: Diagnosis, and pharmacological and psychosocial management. *Lancet Neurol.* **9**, 77–93.
- Butler-Browne, G. S., Barbet, J. P., and Thornell, L. E. (1990). Myosin heavy and light chain expression during human skeletal muscle development and precocious muscle maturation induced by thyroid hormone. *Anat. Embryol.* **181**, 513–522.
- Cafforio, P., Dammacco, F., Gernone, A., and Silvestris, F. (2005). Statins activate the mitochondrial pathway of apoptosis in human lymphoblasts and myeloma cells. *Carcinogenesis* **26**, 883–891.
- Casado, E., Gratacos, J., Tolosa, C., Martinez, J. M., Ojanguren, I., Ariza, A., Real, J., Sanjuan, A., and Larrosa, M. (2006). Antimalarial myopathy: An underdiagnosed complication? Prospective longitudinal study of 119 patients. *Ann. Rheum. Dis.* **65**, 385–390.
- Castillero, E., Alamdari, N., Lecker, S. H., and Hasselgren, P. O. (2013). Suppression of atrogin-1 and murf1 prevents dexamethasone-induced atrophy of cultured myotubes. *Metabolism* **62**, 1495–1502.
- Castro, C., and Gourley, M. (2012). Diagnosis and treatment of inflammatory myopathy: Issues and management. *Ther. Adv. Musculoskelet. Dis.* **4**, 111–120.
- Chavez, L. O., Leon, M., Einav, S., and Varon, J. (2016). Beyond muscle destruction: A systematic review of rhabdomyolysis for clinical practice. *Crit. Care* **20**, 135.
- Chen, X., and Li, Y. (2009). Role of matrix metalloproteinases in skeletal muscle: Migration, differentiation, regeneration and fibrosis. *Cell Adh. Migr.* **3**, 337–341.
- Chen, Y. H., Chen, Y. C., Liu, C. S., and Hsieh, M. C. (2016). The different effects of atorvastatin and pravastatin on cell death and parp activity in pancreatic nit-1 cells. *J. Diabetes Res.* **2016**, 1–17.
- Conklin, L. S., Damsker, J. M., Hoffman, E. P., Jusko, W. J., Mavroudis, P. D., Schwartz, B. D., Mengle-Gaw, L. J., Smith, E. C., Mah, J. K., Guglieri, M., et al. (2018). Phase IIA trial in Duchenne muscular dystrophy shows vamorolone is a first-in-class dissociative steroidal anti-inflammatory drug. *Pharmacol. Res.* **136**, 140–150.
- Corsini, A., Bellosta, S., Baetta, R., Fumagalli, R., Paoletti, R., and Bernini, F. (1999). New insights into the pharmacodynamic and pharmacokinetic properties of statins. *Pharmacol. Ther.* **84**, 413–428.
- Dabby, R., Sadeh, M., Herman, O., Berger, E., Watemberg, N., Hayek, S., Jossiphov, J., and Nevo, Y. (2006). Asymptomatic or minimally symptomatic hyperckemia: Histopathologic correlates. *Isr. Med. Assoc. J.* **8**, 110–113.
- Dalakas, M. C., Illa, I., Pezeshkpour, G. H., Laukaitis, J. P., Cohen, B., and Griffin, J. L. (1990). Mitochondrial myopathy caused by long-term zidovudine therapy. *N. Engl. J. Med.* **322**, 1098–1105.
- Davis, B. N., Santoso, J. W., Walker, M. J., Cheng, C. S., Koves, T. R., Kraus, W. E., and Truskey, G. A. (2017). Human, tissue-engineered, skeletal muscle myobundles to measure oxygen uptake and assess mitochondrial toxicity. *Tissue Eng. Part C Methods* **23**, 189–199.
- Delaporte, C., Dautreux, B., and Fardeau, M. (1986). Human myotube differentiation in vitro in different culture conditions. *Biol. Cell* **57**, 17–22.
- Dixon, R. W., and Harris, J. B. (1996). Myotoxic activity of the toxic phospholipase, notexin, from the venom of the Australian tiger snake. *J. Neuropathol. Exp. Neurol.* **55**, 1230–1237.
- Escobar, Y., Venturelli, C. R., and Hoyo-Vadillo, C. (2005). Pharmacokinetic properties of pravastatin in Mexicans: An open-label study in healthy adult volunteers. *Curr. Ther. Res. Clin. Exp.* **66**, 238–246.
- Funanage, V. L., Smith, S. M., and Minnich, M. A. (1992). Entactin promotes adhesion and long-term maintenance of cultured regenerated skeletal myotubes. *J. Cell Physiol.* **150**, 251–257.
- Gholobova, D., Decroix, L., Van Muylder, V., Desender, L., Gerard, M., Carpentier, G., Vandeburgh, H., and Thorrez, L. (2015). Endothelial network formation within human tissue-engineered skeletal muscle. *Tissue Eng. Part A* **21**, 2548–2558.
- Godoy, J. C., Niesman, I. R., Busija, A. R., Kassan, A., Schilling, J. M., Schwarz, A., Alvarez, E. A., Dalton, N. D., Drummond, J. C., Roth, D. M., et al. (2019). Atorvastatin, but not pravastatin, inhibits cardiac akt/mTOR signaling and disturbs mitochondrial ultrastructure in cardiac myocytes. *FASEB J.* **33**, 1209–1225.
- Goldstein, R. A. (2017). Skeletal muscle injury biomarkers: Assay qualification efforts and translation to the clinic. *Toxicol. Pathol.* **45**, 943–951.
- Govoni, A., Magri, F., Brajkovic, S., Zanetta, C., Faravelli, I., Corti, S., Bresolin, N., and Comi, G. P. (2013). Ongoing therapeutic trials and outcome measures for Duchenne muscular dystrophy. *Cell. Mol. Life Sci.* **70**, 4585–4602.
- Gueugneau, M., d'Hose, D., Barbé, C., de Barsy, M., Lause, P., Maiter, D., Bindels, L. B., Delzenne, N. M., Schaeffer, L., Gangloff, Y.-G., et al. (2018). Increased serpinA3n release into circulation during glucocorticoid-mediated muscle atrophy. *J. Cachexia Sarcopenia Muscle* **9**, 929–946.
- Gunasekaran, P. M., Luther, J. M., and Byrd, J. B. (2019). For what factors should we normalize urinary extracellular mRNA biomarkers? *Biomol. Detect. Quantif.* **17**, 100090.
- Gunst, J. J., Langlois, M. R., Delanghe, J. R., De Buyzere, M. L., and Leroux-Roels, G. G. (1998). Serum creatine kinase activity is not a reliable marker for muscle damage in conditions associated with low extracellular glutathione concentration. *Clin. Chem.* **44**, 939–943.
- Gupta, A., and Gupta, Y. (2013). Glucocorticoid-induced myopathy: Pathophysiology, diagnosis, and treatment. *Indian J. Endocrinol. Metab.* **17**, 913–916.
- Hamalainen, N., and Pette, D. (1997). Coordinated fast-to-slow transitions of myosin and serca isoforms in chronically stimulated muscles of euthyroid and hyperthyroid rabbits. *J. Muscle Res. Cell Motil.* **18**, 545–554.
- Hathout, Y., Brody, E., Clemens, P. R., Cripe, L., DeLisle, R. K., Furlong, P., Gordish-Dressman, H., Hache, L., Henricson, E., Hoffman, E. P., et al. (2015). Large-scale serum protein biomarker discovery in Duchenne muscular dystrophy. *Proc. Natl. Acad. Sci. U.S.A.* **112**, 7153–7158.

- Hathout, Y., Conklin, L. S., Seol, H., Gordish-Dressman, H., Brown, K. J., Morgenroth, L. P., Nagaraju, K., Heier, C. R., Damsker, J. M., van den Anker, J. N., et al. (2016a). Serum pharmacodynamic biomarkers for chronic corticosteroid treatment of children. *Sci. Rep.* **6**, 31727.
- Hathout, Y., Seol, H., Han, M. H., Zhang, A., Brown, K. J., and Hoffman, E. P. (2016b). Clinical utility of serum biomarkers in Duchenne muscular dystrophy. *Clin. Proteomics* **13**, 9.
- Hay, M., Thomas, D. W., Craighead, J. L., Economides, C., and Rosenthal, J. (2014). Clinical development success rates for investigational drugs. *Nat. Biotechnol.* **32**, 40–51.
- Hinds, S., Bian, W., Dennis, R. G., and Bursac, N. (2011). The role of extracellular matrix composition in structure and function of bioengineered skeletal muscle. *Biomaterials* **32**, 3575–3583.
- Jacquemin, V., Furling, D., Bigot, A., Butler-Browne, G. S., and Mouly, V. (2004). Igf-1 induces human myotube hypertrophy by increasing cell recruitment. *Exp. Cell Res.* **299**, 148–158.
- Jesinkey, S. R., Korrapati, M. C., Rasbach, K. A., Beeson, C. C., and Schnellmann, R. G. (2014). Atomoxetine prevents dexamethasone-induced skeletal muscle atrophy in mice. *J. Pharmacol. Exp. Ther.* **351**, 663–673.
- Juhas, M., Abutaleb, N., Wang, J. T., Ye, J., Shaikh, Z., Sriworarat, C., Qian, Y., and Bursac, N. (2018). Incorporation of macrophages into engineered skeletal muscle enables enhanced muscle regeneration. *Nat. Biomed. Eng.* **2**, 942–954.
- Juhas, M., Engelmayer, G. C., Jr, Fontanella, A. N., Palmer, G. M., and Bursac, N. (2014). Biomimetic engineered muscle with capacity for vascular integration and functional maturation in vivo. *Proc. Natl. Acad. Sci. U.S.A.* **111**, 5508–5513.
- Kaufmann, P., Torok, M., Zahno, A., Waldhauser, K. M., Brecht, K., and Krahenbuhl, S. (2006). Toxicity of statins on rat skeletal muscle mitochondria. *Cell. Mol. Life Sci.* **63**, 2415–2425.
- Keltz, E., Khan, F. Y., and Mann, G. (2014). Rhabdomyolysis. The role of diagnostic and prognostic factors. *Muscles Ligaments Tendons J.* **03**, 303–312.
- Khaleeli, A. A., Edwards, R. H., Gohil, K., McPhail, G., Rennie, M. J., Round, J., and Ross, E. J. (1983). Corticosteroid myopathy: A clinical and pathological study. *Clin. Endocrinol. (Oxf.)* **18**, 155–166.
- Khodabukus, A., Madden, L., Prabhu, N. K., Koves, T. R., Jackman, C. P., Muoio, D. M., and Bursac, N. (2019). Electrical stimulation increases hypertrophy and metabolic flux in tissue-engineered human skeletal muscle. *Biomaterials* **198**, 259–269.
- Khodabukus, A., Prabhu, N., Wang, J., and Bursac, N. (2018). In vitro tissue-engineered skeletal muscle models for studying muscle physiology and disease. *Adv. Healthcare Mater.* **7**, e1701498.
- Kim, J. W., Ku, S. K., Han, M. H., Kim, K. Y., Kim, S. G., Kim, G. Y., Hwang, H. J., Kim, B. W., Kim, C. M., and Choi, Y. H. (2015). The administration of *Fructus Schisandrae* attenuates dexamethasone-induced muscle atrophy in mice. *Int. J. Mol. Med.* **36**, 29–42.
- Larkin, L. M., Van der Meulen, J. H., Dennis, R. G., and Kennedy, J. B. (2006). Functional evaluation of nerve-skeletal muscle constructs engineered in vitro. *In Vitro Cell. Dev. Biol. Anim.* **42**, 75–82.
- Lee, M. K., Choi, J. W., Choi, Y. H., and Nam, T. J. (2018). Pyropia yezoensis protein supplementation prevents dexamethasone-induced muscle atrophy in c57bl/6 mice. *Mar. Drugs* **16**, e328.
- Madden, L., Juhas, M., Kraus, W. E., Truskey, G. A., and Bursac, N. (2015). Bioengineered human myobundles mimic clinical responses of skeletal muscle to drugs. *Elife* **4**, e04885.
- Maffioletti, S. M., Sarcar, S., Henderson, A. B. H., Mannhardt, I., Pinton, L., Moyle, L. A., Steele-Stallard, H., Cappellari, O., Wells, K. E., Ferrari, G., et al. (2018). Three-dimensional human iPSC-derived artificial skeletal muscles model muscular dystrophies and enable multilineage tissue engineering. *Cell Rep.* **23**, 899–908.
- Maji, D., Shaikh, S., Solanki, D., and Gaurav, K. (2013). Safety of statins. *Indian J. Endocrinol. Metab.* **17**, 636–646.
- Maliver, P., Festag, M., Bennecke, M., Christen, F., Banfai, B., Lenz, B., and Winter, M. (2017). Assessment of preclinical liver and skeletal muscle biomarkers following clofibrate administration in Wistar rats. *Toxicol. Pathol.* **45**, 506–525.
- Meor Anuar Shuhaili, M. F. R., Samsudin, I. N., Stanslas, J., Hasan, S., and Thambiah, S. C. (2017). Effects of different types of statins on lipid profile: A perspective on Asians. *Int. J. Endocrinol. Metab.* **15**, e43319.
- Mills, R. J., Parker, B. L., Monnot, P., Needham, E. J., Vivien, C. J., Ferguson, C., Parton, R. G., James, D. E., Porrello, E. R., and Hudson, J. E. (2019). Development of a human skeletal muscle platform with pacing capabilities. *Biomaterials* **198**, 217–227.
- Minetto, M. A., Botter, A., Lanfranco, F., Baldi, M., Ghigo, E., and Arvat, E. (2010). Muscle fiber conduction slowing and decreased levels of circulating muscle proteins after short-term dexamethasone administration in healthy subjects. *J. Clin. Endocrinol. Metab.* **95**, 1663–1671.
- Mozaffar, T., Haddad, F., Zeng, M., Zhang, L. Y., Adams, G. R., and Baldwin, K. M. (2007). Molecular and cellular defects of skeletal muscle in an animal model of acute quadriplegic myopathy. *Muscle Nerve* **35**, 55–65.
- Muck, W., Frey, R., Unger, S., and Voith, B. (2000). Pharmacokinetics of cerivastatin when administered under fasted and fed conditions in the morning or evening. *Int. J. Clin. Pharmacol. Ther.* **38**, 298–303.
- Muck, W., Unger, S., Kawano, K., and Ahr, G. (1998). Inter-ethnic comparisons of the pharmacokinetics of the HMG-CoA reductase inhibitor cerivastatin. *Br. J. Clin. Pharmacol.* **45**, 583–590.
- Musaro, A., and Rosenthal, N. (1999). Maturation of the myogenic program is induced by postmitotic expression of insulin-like growth factor I. *Mol. Cell. Biol.* **19**, 3115–3124.
- Oleaga, C., Bernabini, C., Smith, A. S., Srinivasan, B., Jackson, M., McLamb, W., Platt, V., Bridges, R., Cai, Y., Santhanam, N., et al. (2016). Multi-organ toxicity demonstration in a functional human in vitro system composed of four organs. *Sci. Rep.* **6**, 20030.
- Omar, M. A., and Wilson, J. P. (2002). FDA adverse event reports on statin-associated rhabdomyolysis. *Ann. Pharmacother.* **36**, 288–295.
- Orzechowski, A., Ostaszewski, P., Wilczak, J., Jank, M., Balasinska, B., Wareski, P., and Fuller, J. Jr (2002). Rats with a glucocorticoid-induced catabolic state show symptoms of oxidative stress and spleen atrophy: The effects of age and recovery. *J. Vet. Med. A Physiol. Pathol. Clin. Med.* **49**, 256–263.
- Osaki, T., Uzel, S. G. M., and Kamm, R. D. (2018). Microphysiological 3d model of amyotrophic lateral sclerosis (ALS) from human IPS-derived muscle cells and optogenetic motor neurons. *Sci. Adv.* **4**, eaat5847.
- Pons, F., Damadei, A., and Leger, J. J. (1987). Expression of myosin light chains during fetal development of human skeletal muscle. *Biochem. J.* **243**, 425–430.
- Powell, C. A., Smiley, B. L., Mills, J., and Vandenburg, H. H. (2002). Mechanical stimulation improves tissue-engineered human skeletal muscle. *Am. J. Physiol. Cell Physiol.* **283**, C1557–1565.

- Quattrocchi, M., Barefield, D. Y., Warner, J. L., Vo, A. H., Hadhazy, M., Earley, J. U., Demonbreun, A. R., and McNally, E. M. (2017). Intermittent glucocorticoid steroid dosing enhances muscle repair without eliciting muscle atrophy. *J. Clin. Invest.* **127**, 2418–2432.
- Queckenberg, C., Wachall, B., Erlinghagen, V., Di Gion, P., Tomalik-Scharfe, D., Tawab, M., Gerbeth, K., and Fuhr, U. (2011). Pharmacokinetics, pharmacodynamics, and comparative bioavailability of single, oral 2-mg doses of dexamethasone liquid and tablet formulations: A randomized, controlled, crossover study in healthy adult volunteers. *Clin. Ther.* **33**, 1831–1841.
- Rabkin, R., Fervenza, F. C., Maidment, H., Ike, J., Hintz, R., Liu, F., Bloedow, D. C., Hoffman, A. R., and Gesundheit, N. (1996). Pharmacokinetics of insulin-like growth factor-1 in advanced chronic renal failure. *Kidney Int.* **49**, 1134–1140.
- Rajashree, S., and Puvanakrishnan, R. (1998). Dexamethasone induced alterations in enzymatic and nonenzymatic antioxidant status in heart and kidney of rats. *Mol. Cell. Biochem.* **181**, 77–85.
- Rangarajan, S., Madden, L., and Bursac, N. (2014). Use of flow, electrical, and mechanical stimulation to promote engineering of striated muscles. *Ann. Biomed. Eng.* **42**, 1391–1405.
- Rao, L., Qian, Y., Khodabukus, A., Ribar, T., and Bursac, N. (2018). Engineering human pluripotent stem cells into a functional skeletal muscle tissue. *Nat. Commun.* **9**, 126.
- Rittoo, D., Jones, A., Lecky, B., and Neithercut, D. (2014). Elevation of cardiac troponin T, but not cardiac troponin I, in patients with neuromuscular diseases: Implications for the diagnosis of myocardial infarction. *J. Am. Coll. Cardiol.* **63**, 2411–2420.
- Rochkind, S., and Shainberg, A. (2017). Muscle response to complete peripheral nerve injury: Changes of acetylcholine receptor and creatine kinase activity over time. *J. Reconstr. Microsurg.* **33**, 352–357.
- Rodrigues, B. M., Dantas, E., de Salles, B. F., Miranda, H., Koch, A. J., Willardson, J. M., and Simao, R. (2010). Creatine kinase and lactate dehydrogenase responses after upper-body resistance exercise with different rest intervals. *J. Strength Cond. Res.* **24**, 1657–1662.
- Rommel, C., Bodine, S. C., Clarke, B. A., Rossman, R., Nunez, L., Stitt, T. N., Yancopoulos, G. D., and Glass, D. J. (2001). Mediation of IGF-1-induced skeletal myotube hypertrophy by pi(3)k/akt/mtor and pi(3)k/akt/gsk3 pathways. *Nat. Cell Biol.* **3**, 1009–1013.
- Rouleau, G., Karpati, G., Carpenter, S., Soza, M., Prescott, S., and Holland, P. (1987). Glucocorticoid excess induces preferential depletion of myosin in denervated skeletal muscle fibers. *Muscle Nerve* **10**, 428–438.
- Sayers, S. P., Clarkson, P. M., and Lee, J. (2000). Activity and immobilization after eccentric exercise: II. Serum ck. *Med. Sci. Sports Exerc.* **32**, 1593–1597.
- Schakman, O., Kalista, S., Barbe, C., Loumaye, A., and Thissen, J. P. (2013). Glucocorticoid-induced skeletal muscle atrophy. *Int. J. Biochem Cell Biol.* **45**, 2163–2172.
- Selvaraj, S., Mondragon-Gonzalez, R., Xu, B., Magli, A., Kim, H., Laine, J., Kiley, J., McKee, H., Rinaldi, F., Aho, J., et al. (2019). Screening identifies small molecules that enhance the maturation of human pluripotent stem cell-derived myotubes. *Elife* **8**.
- Sharp, N. J., Kornegay, J. N., Bartlett, R. J., Hung, W. Y., and Dykstra, M. J. (1993). Notexin-induced muscle injury in the dog. *J. Neurol. Sci.* **116**, 73–81.
- Shimizu, K., Genma, R., Gotou, Y., Nagasaka, S., and Honda, H. (2017). Three-dimensional culture model of skeletal muscle tissue with atrophy induced by dexamethasone. *Bioengineering (Basel)* **4**, 56.
- Shimizu, N., Yoshikawa, N., Ito, N., Maruyama, T., Suzuki, Y., Takeda, S., Nakae, J., Tagata, Y., Nishitani, S., Takehana, K., et al. (2011). Crosstalk between glucocorticoid receptor and nutritional sensor mtor in skeletal muscle. *Cell Metab.* **13**, 170–182.
- Si, Y., Cui, X., Crossman, D. K., Hao, J., Kazamel, M., Kwon, Y., and King, P. H. (2018). Muscle microrna signatures as biomarkers of disease progression in amyotrophic lateral sclerosis. *Neurobiol. Dis.* **114**, 85–94.
- Siracusa, J., Koulmann, N., and Banzet, S. (2018). Circulating myomirs: A new class of biomarkers to monitor skeletal muscle in physiology and medicine. *J. Cachexia Sarcopenia Muscle* **9**, 20–27.
- Skardal, A., Murphy, S. V., Devarasetty, M., Mead, I., Kang, H. W., Seol, Y. J., Shrike Zhang, Y., Shin, S. R., Zhao, L., Aleman, J., et al. (2017). Multi-tissue interactions in an integrated three-tissue organ-on-a-chip platform. *Sci. Rep.* **7**, 8837.
- Song, S. E., Shin, S. K., Park, S. Y., Hwang, I. S., Im, S. S., Bae, J. H., Choi, M. S., and Song, D. K. (2018). Epac2a-knockout mice are resistant to dexamethasone-induced skeletal muscle atrophy and short-term cold stress. *BMB Rep.* **51**, 39–44.
- Spoorenberg, S. M., Deneer, V. H., Grutters, J. C., Pulles, A. E., Voorn, G. P., Rijkers, G. T., Bos, W. J., and van de Garde, E. M. (2014). Pharmacokinetics of oral vs. intravenous dexamethasone in patients hospitalized with community-acquired pneumonia. *Br. J. Clin. Pharmacol.* **78**, 78–83.
- Staffa, J. A., Chang, J., and Green, L. (2002). Cerivastatin and reports of fatal rhabdomyolysis. *N. Engl. J. Med.* **346**, 539–540.
- Stamenkovic, I. (2003). Extracellular matrix remodelling: The role of matrix metalloproteinases. *J. Pathol.* **200**, 448–464.
- Thankamony, A., Capalbo, D., Marcovecchio, M. L., Sleight, A., Jorgensen, S. W., Hill, N. R., Mooslehner, K., Yeo, G. S., Bluck, L., Juul, A., et al. (2014). Low circulating levels of IGF-1 in healthy adults are associated with reduced beta-cell function, increased intramyocellular lipid, and enhanced fat utilization during fasting. *J. Clin. Endocrinol. Metab.* **99**, 2198–2207.
- Thompson, P. D., Clarkson, P., and Karas, R. H. (2003). Statin-associated myopathy. *JAMA* **289**, 1681–1690.
- Tiburcy, M., Markov, A., Kraemer, L. K., Christalla, P., Rave-Fraenk, M., Fischer, H. J., Reichardt, H. M., and Zimmermann, W. H. (2019). Regeneration competent satellite cell niches in rat engineered skeletal muscle. *FASEB Bioadv.* **1**, 731–746.
- Tonomura, Y., Matsushima, S., Kashiwagi, E., Fujisawa, K., Takagi, S., Nishimura, Y., Fukushima, R., Torii, M., and Matsubara, M. (2012). Biomarker panel of cardiac and skeletal muscle troponins, fatty acid binding protein 3 and myosin light chain 3 for the accurate diagnosis of cardiotoxicity and musculoskeletal toxicity in rats. *Toxicology* **302**, 179–189.
- Torres, P. A., Helmstetter, J. A., Kaye, A. M., and Kaye, A. D. (2015). Rhabdomyolysis: Pathogenesis, diagnosis, and treatment. *Ochsner J.* **15**, 58–69.
- Vaananen, H. K., Takala, T. E., Tolonen, U., Vuori, J., and Myllyla, V. V. (1988). Muscle-specific carbonic anhydrase III is a more sensitive marker of muscle damage than creatine kinase in neuromuscular disorders. *Arch. Neurol.* **45**, 1254–1256.
- Vandenburgh, H., Shansky, J., Benesch-Lee, F., Barbata, V., Reid, J., Thorrez, L., Valentini, R., and Crawford, G. (2008). Drug-screening platform based on the contractility of tissue-engineered muscle. *Muscle Nerve* **37**, 438–447.
- Vernetti, L., Gough, A., Baetz, N., Blutt, S., Broughman, J. R., Brown, J. A., Foulke-Abel, J., Hasan, N., In, J., Kelly, E., et al. (2017). Functional coupling of human microphysiology

- systems: Intestine, liver, kidney proximal tubule, blood-brain barrier and skeletal muscle. *Sci. Rep.* **7**, 42296.
- Vila, O. F., Uzel, S. G. M., Ma, S. P., Williams, D., Pak, J., Kamm, R. D., and Vunjak-Novakovic, G. (2019). Quantification of human neuromuscular function through optogenetics. *Theranostics* **9**, 1232–1246.
- Waddell, D. S., Baehr, L. M., van den Brandt, J., Johnsen, S. A., Reichardt, H. M., Furlow, J. D., and Bodine, S. C. (2008). The glucocorticoid receptor and foxo1 synergistically activate the skeletal muscle atrophy-associated murf1 gene. *Am. J. Physiol. Endocrinol. Metab.* **295**, E785–E797.
- Wang, J., Khodabukus, A., Rao, L., Vandusen, K., Abutaleb, N., and Bursac, N. (2019). Engineered skeletal muscles for disease modeling and drug discovery. *Biomaterials* **221**, 119416.
- Washabaugh, C. H., Ontell, M. P., Kant, J. A., Daood, M. J., Watchko, J. F., Watkins, S. C., and Ontell, M. (2001). Effect of chronic denervation and denervation-reinnervation on cytoplasmic creatine kinase transcript accumulation. *J. Neurobiol.* **47**, 194–206.
- Westwood, F. R., Bigley, A., Randall, K., Marsden, A. M., and Scott, R. C. (2005). Statin-induced muscle necrosis in the rat: Distribution, development, and fibre selectivity. *Toxicol. Pathol.* **33**, 246–257.
- Xu, Z., Feng, X., Dong, J., Wang, Z. M., Lee, J., Furdui, C., Files, D. C., Beavers, K. M., Kritchevsky, S., Milligan, C., et al. (2017). Cardiac troponin t and fast skeletal muscle denervation in ageing. *J. Cachexia Sarcopenia Muscle* **8**, 808–823.
- Zhang, X., Hong, S., Yen, R., Kondash, M., Fernandez, C. E., and Truskey, G. A. (2018). A system to monitor statin-induced myopathy in individual engineered skeletal muscle myobundles. *Lab. Chip* **18**, 2787–2796.